Journal of Hip Preservation Surgery Vol. 4, No. 4, pp. 276–288
doi: 10.1093/jhps/hnx030
Advance Access Publication 14 September 2017
Review article

Preoperative planning for redirective, periacetabular osteotomies

Christoph E. Albers[1,2*], Piet Rogers[1], Nicholas Wambeek[3], Sufian S. Ahmad[2], Piers J. Yates[1,4] and Gareth H. Prosser[1,4]

[1]Department of Orthopaedic Surgery, Fremantle and Fiona Stanley Hospitals, 11 Robin Warren Dr, Murdoch, WA 6150, Australia,
[2]Department of Orthopaedic Surgery, University Hospital Bern, Freiburgstr. 4, 3010 Bern, Switzerland,
[3]Department of Radiology, Fremantle and Fiona Stanley Hospitals, 11 Robin Warren Dr, Murdoch, WA 6150, Australia and
[4]Faculty of Medicine, Dentistry and Health Science, University of Western Australia, 35 Stirling Hwy, Crawley WA 6009, Australia
*Correspondence to: C. E. Albers. E-mail: christoph.e.albers@gmail.com
Submitted 3 January 2017; Revised 27 June 2017; revised version accepted 30 July 2017

ABSTRACT

Redirective, periacetabular osteotomies (PAO) represent a group of surgical procedures for treatment of developmental dysplasia of the hip (DDH) in skeletally mature and immature patients. The ultimate goal of all procedures is to reduce symptoms, improve function and delay or prevent progression of osteoarthritis. During the last two decades, the understanding of the underlying pathomechanisms has continuously evolved. This is mainly attributable to the development of the femoroacetabular impingement concept that has increased the awareness of the underlying three-dimensional complexity associated with DDH. With increasing knowledge about the pathobiomechanics of dysplastic hips, diagnostic tools have improved allowing for sophisticated preoperative analyses of the morphological and pathobiomechanical features, and early recognition of degenerative changes, which may alter the long-term outcome. As redirective, PAO are technically demanding procedures, preoperative planning is crucial to avoid intraoperative obstacles and to sufficiently address the patient-specific deformity. Although conventional radiography has been used for decades, it has not lost its primary role in the diagnostic work-up of patients with DDH. Furthermore, an increasing number of modern imaging techniques exists allowing for assessment of early cartilage degeneration (biochemical magnetic resonance imaging) as well as 3D planning and computer-based virtual treatment simulation of PAO. This article reviews the literature with regard to the current concepts of imaging of DDH, preoperative planning and treatment recommendations for redirective, PAO.

INTRODUCTION

The natural course of developmental dysplasia of the hip (DDH) has been reported to be poor, with early development of osteoarthritis (OA) requiring joint replacement surgery [1–4]. Depending on the patient's age and skeletal maturity, different pelvic osteotomies have been proposed to surgically treat this condition. All techniques aim at improving hip pain and function by addressing the abnormal biomechanics of the hip. The goal is to relieve pain and to delay or prevent progression of OA to preserve the natural hip joint over time. Generally, pelvic osteotomies can be categorized as augmentation procedures and reorientation procedures. Augmentation procedures include shelf osteotomies [5], the Salter osteotomy [6] and the Chiari osteotomy [7]. Redirective, periacetabular osteotomies (PAO) include rotational/spherical osteotomies [8, 9], triple osteotomies [10, 11] and the Bernese PAO [12]. The general principles for preoperative planning do not differ among the different types of PAOs. However, most of recently published studies related to preoperative radiographic planning for redirective PAOs refer to the Bernese PAO. Therefore, direct implementation of the here listed planning principles should be done with caution when performing spherical/rotational or triple osteotomies. Skeletal maturity is a prerequisite when performing the Bernese PAO or spherical/rotational procedures as the osteotomies cross the triradiate cartilage complex in skeletally immature

patients and may lead to early acetabular growth arrest and joint incongruency. This does not apply to triple osteotomies as the growth plates of the innominate bone remain uncompromised making triple osteotomies the procedure of choice in skeletally immature patients. PAOs render the potential of a free 3D re-orientation of the acetabulum. Due to the ability of performing an almost unlimited re-orientation in the spatial room, severe dysplastic deformities [13, 14] and other complex hip deformities such as sequelae of Legg Calve Perthes disease [15, 16] or proximal femoral deficiency [17] can be treated with redirective, PAO. Additionally, acetabular retroversion causing pincer-type impingement can be corrected when performing an anteverting PAO [18, 19]. However, PAO are technically demanding procedures that are prone to treatment errors and complications if performed without adequate expertise. Patient selection, correct indication and thorough preoperative planning are crucial for successful outcome. The current article reviews the literature highlighting preoperative 2D and 3D imaging tools for preoperative planning of redirective, PAO.

BACKGROUND

DDH has been classically defined as deficient anterolateral acetabular coverage with a decreased surface area of the acetabular, articular surface and a steep orientation of the acetabular roof [20]. The radius of the acetabular curvature frequently exceeds that of the femoral head resulting in joint incongruency (sloping roof dysplasia) [21]. Short- or flat-roof dysplasia, in contrast, is represented by normal inclination of the acetabulum, whereas overall femoral head coverage is reduced [21, 22]. Short- or flat-roof dysplasia has been aetiologically attributed to recurrent impingement from an asphericity of the femoral head leading to growth and remodelling abnormalities of the iliac acetabular epiphysis after closure of the triradiate cartilage complex [22]. The forces around the hip concentrate on the edge of the superior acetabular socket resulting in static overload [20, 23]. This condition is aggravated by frequently occurring instability with subluxation of the joint leading to a further increase of the peak pressures onto the articular cartilage particularly in hips with steep roof dysplasia [21]. The resulting intra-articular damage pattern comprises compensatory hypertrophy of the labrum with subsequent partial or complete tears [24], cartilage damage [25–27] and ultimately OA [4]. Short- or flat-roof dysplasia can be associated with osseous fatigue fractures of the superior acetabular margin [21]. Since the widespread recognition of femoroacetabular impingement (FAI) [28], the understanding of the pathological hip biomechanics has evolved. This has increased the awareness of the underlying 3D problem associated with DDH. In this context, DDH was found to be associated with acetabular retroversion [29–31] resulting in a mixed picture of DDH and FAI [32]. Both under-correcting and overcorrecting femoral head coverages were found to predict failure after Bernese PAO [32, 33]. Additionally, it was shown that the articulating surface area of the acetabulum is decreased in dysplastic hips compared with normal hips [34, 35]. The resulting decreased contact area between the acetabulum and the femoral head remains unchanged after PAO. A dysplastic acetabulum can therefore only be corrected as close as possible to a normal acetabulum. Furthermore, surgical treatment of sloping roof dysplasia and short/flat roof dysplasia may vary considerably due to the pathomorphologic differences of these two entities (pelvic osteotomies versus treatment of impingement) [22]. To date, there are no universal guidelines regarding target ranges of specific radiographic parameters to achieve an optimal correction. Alongside preditive factors associated with surgical accuracy (over-/under-correction), further negative predictors of outcome have been identified in previous studies including increased age at surgery, preoperative pain und reduced hip function, pre-existing OA, and hip subluxation [17, 32, 33, 36]. However, this is in contrast to other studies that reported favourable outcomes in older patients and patients with radiographic signs of preoperative OA after rotational/spherical and Bernese PAO [37–39].

CONVENTIONAL IMAGING

Conventional radiography is the primary imaging modality for preoperative planning. The routine preoperative work-up includes an anterior-posterior (AP) radiograph of the pelvis and a lateral projection of the hip [40, 41] (i.e. cross-table view, frog-leg view, Lauenstein view [42], Dunn Rippstein Müller view [43, 44]). A false-profile view [45], a true lateral pelvic view and functional views serve as adjuncts. In the initial study by Ganz *et al.* [12], the authors suggested an AP view of the pelvis, a false-profile view, and abduction views as the minimally required preoperative projections for the Bernese PAO. However, they noted that computed tomography might add to a more precise 3D planning [12, 46]. It must be emphasized that despite the increasing availability of modern imaging technologies, conventional radiography has not lost its role in the preoperative work-up of dysplastic hips and remains a mandatory imaging tool for the assessment of DDH, treatment planning and postoperative evaluation of the achieved correction. Furthermore, the majority of radiographic factors (pre- and postoperatively) predicting outcome after PAO

have been identified and validated on conventional radiographs [17, 32, 33, 36].

A variety of radiographic parameters associated with DDH exist to assess femoral head coverage, orientation of the acetabulum, joint congruity, femoral head sphericity, femoral torsion and the neck shaft angle (Table I). On the AP pelvis radiograph, lateral acetabular coverage is assessed by the lateral center edge angle (LCE [20]), the acetabular index (AI [47]) and extrusion index (EI [1]; Figs.1 and 2). Anterior femoral head coverage can be assessed with the anterior CE [45] on the false-profile view and the anterior acetabular wall index [48] on the AP pelvis radiograph. Posterior coverage and acetabular version are assessed by the presence or absence of posterior wall sign [31] (Fig. 1), a crossover sign [31], the ischial spine sign [49], the retroversion index (RI) [40] and the posterior acetabular wall index [48] on the AP pelvic radiograph. A previous study suggested reference values for acetabular over- and undercoverage on the AP pelvis radiograph obtained in a standardized fashion with standardized pelvic tilt and rotation (Table I) [19]. Eleven common radiographic parameters in patients with hip dysplasia undergoing PAO ($n = 26$), isolated cam type FAI and isolated pincer-type FAI undergoing surgical hip dislocation were assessed. The intersection of the distribution curves determined the threshold values for each parameter (Table I).

Standardized acquisition techniques of plain radiographs are of upmost importance as factors such as film-tube distance, patient-film distance, centring and direction of the X-ray beam and pelvic orientation [50–55]. Most radiographic parameters of the hip have been defined on AP pelvic radiographs with the central beam directed to the radiographic centre of the pelvis defined as the midpoint between upper border of symphysis and midpoint between anterior superior iliac spines [40]. Interpreting radiographic parameters on different projections such as low centred AP pelvis projections, hip centred projections or fluoroscopic images should be performed with caution because the projected angles can vary significantly from the standardized AP pelvis radiograph [54]. Pelvic orientation during image acquisition (i.e. pelvic tilt, rotation and obliquity) has considerable effects on many radiographic parameters associated with DDH [51, 53, 56]. A previous study investigated the effects of tilt and rotation on a selection of standard radiographic parameters [51] and found anterior and posterior acetabular coverage [52, 57], the crossover and posterior wall sign [31] and the RI [40, 51] to vary considerably, whereas the LCE [20], AI [58], EI [1], ACM angle [59], Sharp angle and craniocaudal coverage [52, 57] were independent of pelvic tilt and orientation [51]. Furthermore, it was reported that pelvic tilt is increased in supine AP pelvic radiographs compared with standing AP pelvic radiographs resulting in differences of the projected acetabular version, whereas the LCE angle remained unchanged [60].

Notably, due to the decreased area of the acetabular articular surface in dysplastic hips, meeting these reference values for normal acetabula after PAO is rarely possible. For instance, normalizing the AI to neutral does not always completely correct the LCE to a normal range. While further abduction would increase the LCE, this may result in a negative AI leading to pincer-type FAI [61]. A previous study revealed that only 6% of hips undergoing PAO for DDH met the previously determined normal ranges of six predefined radiographic parameters (LCE, AI, EI, computerized anterior, posterior and total coverage) [32]. Optimal acetabular reorientation was therefore defined if at least four of these six parameters were in the normal range resulting in improved survivorship after 10-year follow-up [32].

Joint congruity is assessed on the AP pelvis radiograph. The distance of the most medial contour of the femoral head to the ilioischial line has been shown to be 5–15 mm [62]. This distance increases with increasing degree of subluxation. Another indicator for joint incongruity and subluxation is an interrupted Shenton line (Fig. 2) [63]. Abduction views can be used to assess joint incongruity. Due to subluxation in DDH, lateral joint space narrowing is frequently observed on the AP pelvis radiograph. In abduction, normal joint space restores due to a realignment or enlocation of the subluxed hip whereas persistent joint space narrowing is a relative contraindication for surgery because it indicates cartilage damage (Fig. 3). Apart from the assessment of subluxation, abduction views simulate the anticipated degree of acetabular reorientation.

Femoral head asphericity is a frequent feature in dysplastic hips, which can lead to secondary cam type FAI after PAO [64, 65]. It was shown previously that concomitant correction of an asphericity of the femoral head resulted in a better outcome 10 years after PAO [32]. Radiographic parameters for femoral head sphericity include the alpha angle [66], the head-neck offset ratio [40, 66, 67] on lateral projections of the hip and the pistol grip deformity on the AP pelvis radiograph [68]. Further associated pathomorphologies of the femur include concomitant valgus, varus and torsional deformities. Although CT represents the gold standard to assess femoral torsion [69], Dunn Rippstein Müller allow for assessment of femoral torsion [43, 44]. Approximately 10% of patients undergoing PAOs require concomitant proximal femoral osteotomies (PFO) [70]. Ganz *et al* [16] proposed an

Table I. Normal and pathologic values of the described radiographic parameters

Category	*Parameter*	*Projection*	*Normal*	*DDH*	*Description*
Acetabular coverage	LCE angle [°] [20]	AP pelvis	23–33	<22	Angle formed by a vertical line and a line through the centre of the femoral head and the lateral edge of the acetabulur
	AI [°] [58]	AP pelvis	3–13	>14	Angle formed by a horizontal line and a line through the medial and lateral edge of the acetabular roof
	EI [%] [40]	AP pelvis	17–27	>27	Percentage of the femoral head width which is not covered by the acetabulum
	Sharpe angle [°] [117]	AP pelvis	38–42	>43	Angle between a horizontal line and a line connecting the acetabular teardrop with the lateral edge of the acetabulum
	Anterior centre edge (ACE) angle [°] [45]	False-profile	>25	<20	Angle formed by a vertical line and a line through the centre of the femoral head and the anterior edge of the acetabulum (A)
Acetabular orientation	PW sign [31]	AP pelvis	Negative	Often positive	Positive if the PW runs medially of the centre of the femoral head
	Anterior/posterior acetabular wall index [48]	AP pelvis	0.41 (range, 0.30–0.51)	0.28 (range, −0.06 to 0.52)	Ratio of the width of the anterior/posterior acetabular wall measured along the femoral head-neck axis divided by the femoral head radius
	Crossover sign [31]	AP pelvis	Negative	Often positive	Anterior wall crosses the PW
	RI [%] [40]	AP pelvis	0	Not described	Percentage of the retroverted acetabular opening divided by the entire opening
	Ischial spine sign [49]	AP pelvis	Negative	Not described	Positive if the ischial spine is projected medially to the pelvic brim
Head neck sphericity	Alpha angle [°] [66]	Cross-table axial	<50	Often >50	Angle formed by the femoral neck axis and line through the centre of the femoral head and the point where the anterior head-neck contour exceeds the head radius

(Continued)

Table I. (Continued)

Category	*Parameter*	*Projection*	*Normal*	*DDH*	*Description*
	Pistol grip deformity [68]	AP pelvis	—	—	Asphericity of the lateral femoral head-neck junction leads to typical appearance of a pistol grip
	Offset [mm] [40]	Cross-table axial	>10 mm	Not described	Difference between the femoral head radius and the neck radius
	Offset ratio [40]	Cross-table axial	>0.20	Not described	Ratio of offset to the femoral head radius
Joint congruency	Shenton's line [intact/interrupted] [63]	AP pelvis	Intact	Often interrupted	Interrupted if the caudal femoral head-neck contour and the superior boarder of the obturator foramen do not form a harmonic arc
	Lateralization of femoral head [mm] [62]	AP pelvis	5–15	~16	Shortest distance between the medial aspect of the femoral head and the ilioischial line
Additional findings	Femoral torsion [°] [47]	Dunn-Rippstein Müller	15– 20	Not described	Angle formed by the femoral neck and femoral shaft axis
	Neck shaft angle [°] [47]	AP pelvis	126–139	Not described	Angle formed by the femoral neck and femoral shaft axis
	Fovea angle delta [°] [118]	AP pelvis	26 ± 10	Not described	Angle formed by a line through the medial edge of the acetabular roof and the centre of the femoral head and a line through the lateral boarder of the fovea capitis femoris and the centre of the femoral head

Modified according to Steppacher *et al.* [54]; acetabular reference values according to Tannast *et al.* [19]. n.a., not applicable.

algorithm that allows to assess the necessity for concomitant PFO. For hips with a normal joint space and sufficient coverage and congruency on abduction views, isolated PAO is indicated. In case of persistent subluxation on abduction views, the abduction view will be repeated with additional internal rotation. Congruency of the joint indicates PAO with concomitant varus and derotation PFO [16].

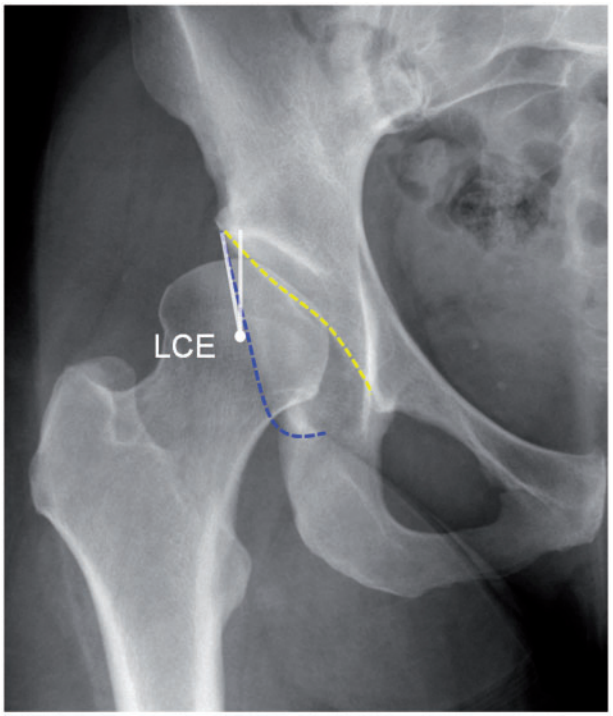

Fig. 1. The right hip of an AP pelvis radiograph of a 22-year-old female patient with symptomatic DDH is shown. The LCE angle (white lines) is 10°. Although acetabular version is correct (negative crossover sign), the PW sign is positive (femoral head centre projecting laterally to the PW [blue dashed]) due to the decreased articular surface area in DDH.

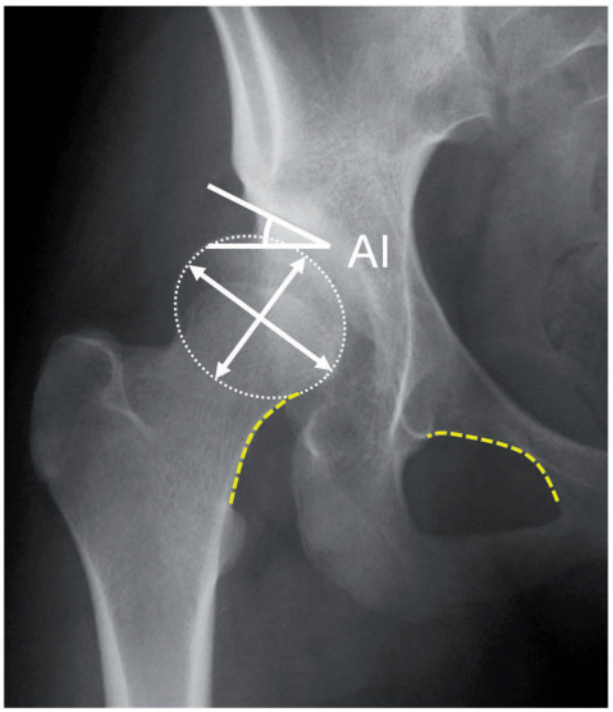

Fig. 2. The right hip of an AP pelvis radiograph of a 28-year-old patient with severe DDH is shown. The acetabular sourcil is steep represented by an increased AI (white lines) of 25°. This has lead to subluxation of the joint, the Shenton's line is interrupted (yellow dashed lines). Additionally, the femoral head is aspherical with an ellipsoid shape (white arrows) [57].

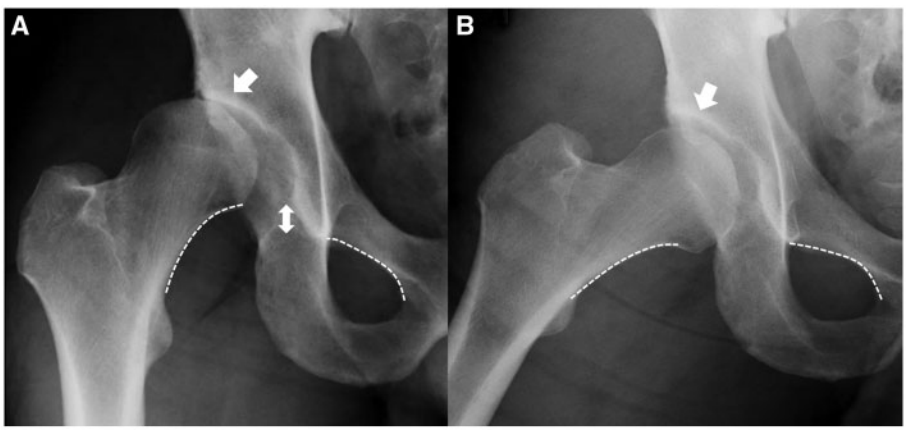

Fig. 3. The right hip of a female patient with DDH is shown. (**A**) The joint is subluxed represented by an interrupted Shenton's line (white dashed line and double arrow) and lateral joint space narrowing (white arrow). (**B**) Abduction of the hip results in joint congruency (intact Shenton's line) and joint space restoration indicating no significant loss of the cartilage layers.

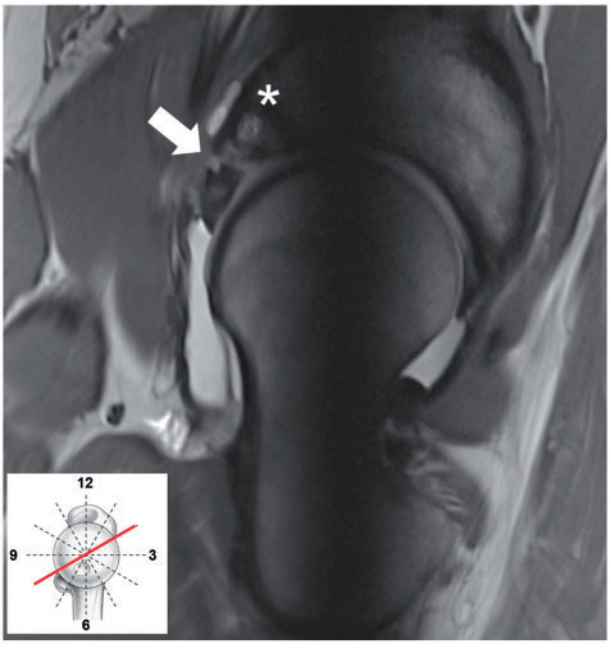

Fig. 4. The radial sequence at the 2 o'clock position of an MR-arthrogram (proton density weighted turbo spin echo sequences at 3 Tesla) of a 24-year-old patient with DDH is shown. Whereas there is no evidence of significant loss of cartilage, the anterosuperior labrum is hypertrophic with hyperintense signal alteration. Additionally, there is a complete undersurface tear of the labrum (white arrow). The adjacent bone reveals cystic lesions due to the static overload in this region (asterisk).

MAGNETIC RESONANCE IMAGING

Magnetic resonance imaging (MRI) (with or without arthrogram) is routinely performed in the preoperative assessment of DDH. MRI allows 3 D assessment of the pathomorphology both on the acetabular and femoral side. The use of intraarticular gadolinium contrast agent injection (MR-arthrogram) has been associated with adverse events such as post injection pain, increased risk of infection and Gadolinium-related local and systemic toxicity [71]. However, despite improving MRI protocols, previous studies revealed higher sensitivity and specificity for the detection of intraarticular cartilaginous and labral lesions on MR-arthrogram as compared with conventional MRI [72, 73]. Radial sequences oriented circumferentially around the femoral neck axis have gained increasing popularity as they provide perpendicular projections of the acetabular wall and labrum at all positions and a circumferential impression of asphericity at the femoral head-neck junction [40]. MRI is useful to detect alterations of the articular cartilage and the acetabular labrum (Fig. 4). A recent multicentre study assessed the status of the labrum in 553 hips undergoing PAO for DDH with concomitant arthrotomy or arthroscopy [74]. Fifty-five percent had a hypertrophic, hypoplastic, or ossified labrum. The prevalence of labral hypertrophy was inversely related to the ACE and LCE. Additionally, 64% of all hips presented with labral tears with the majority being degenerative tears (52%) or detachment (39%) according to the grading system by Beck *et al.* [75], and only 7.2% complete labral avulsions [74]. Leunig *et al.* [24] compared MRI of 14 dysplastic hips and 14 hips with FAI. Of the dysplastic hips, 86% revealed labral hypertrophy while none of the hips with FAI had signs of labral hypertrophy. Thus, the authors concluded that labral hypertrophy is a good predictor for the presence of dysplasia. Another recent study by Garabekyan *et al.* [76] confirmed these findings. Stratified by the degree of the LCE, the authors found increased labral length measured on MRI in hips with frank dysplasia (LCE < 20) and borderline dysplasia (LCE $<25^\circ$ and $>20^\circ$) compared with normal hips and hips with pincer morphology [76]. The authors concluded that labral length may represent an adaptive change in response to instability and serves as a guide for clinical decision making in hips with borderline DDH.

Advanced OA has been reported as an independent risk factor for a poor outcome after PAO [17, 32, 33, 77]. MRI is useful to assess the chondral status. In particular, nonfat-suppressed fast spin echo sequences are often preferred as they provide excellent contrast between bone, cartilage, and joint fluid [78]. Cartilage damage includes full and partial thickness defects. Serial MRI assists in detecting progressive degeneration with chondral hyperintensity and loss of normal grey scale stratification as early signs of degeneration. Often, surface fibrillation is noted prior to more substantial lesions [79].

Biochemical MRI allows to detect joint degeneration at an early stage. As such, delayed gadolinium-enhanced MRI of cartilage (dGEMRIC) is increasingly implemented in the clinical routine (Fig. 5). Loss of glucosaminoglycan (GAG) content in the cartilage is associated with an early change of degenerative joint disease that appears prior to structural damages detected on MRI or plain radiographs [80]. dGEMRIC depicts reduced GAG represented by reduced T1 relaxation times. A previous study showed that a low dGEMRIC index (defined as the average T1 time measured on four femoral and acetabular coronal slices in the weight bearing zone) predicts premature failure after PAO [25]. Regional variations in GAG content in dysplastic hips [81] revealed a higher failure rate after PAO with a low dGEMRIC index in the anterior portion of the joint [27]. Additionally, it was shown that GAG content changes before and after PAO, an observation that was attributed to changed mechanical loading properties of the cartilage [26]. Alongside dGEMRIC, T2-mapping has been

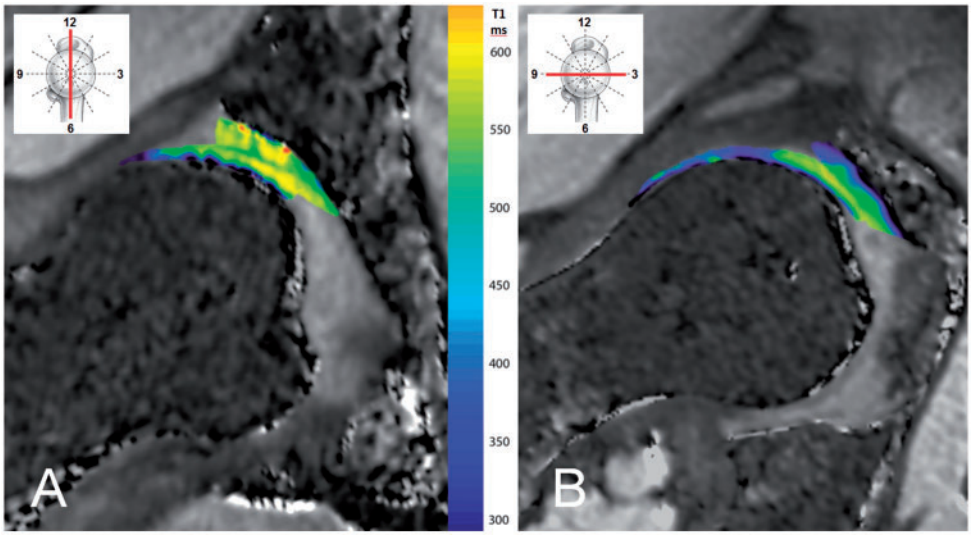

Fig. 5. Biosensitive MRI (dGEMRIC; 3Tesla, i.v. dual-flip angle gradient-echo) of a female patient with DDH is illustrated. Radial sequences rotating around the femoral neck axis reveal regional differences of cartilage quality with (**A**) high GAG content in the superior region (represented by the yellow colour coded increased T1 relaxation time) both of the femoral and acetabular cartilage. (**B**) In the anterior region, GAG content is decreased represented by the blue colour coded decreased T1 relaxation time.

introduced as further biochemical method for identifying cartilage damage based on its composition. Decreased water content and loss of collagen fibre orientation in the cartilage, both of which is found as a sign of early cartilage degeneration, results in increased T2 relaxation times [82, 83]. Hamada *et al.* [84] compared the 3D distribution of acetabular cartilage T2 mapping in nine symptomatic patients with DDH (mean LCE = 5°) without radiographic signs of OA to those from asymptomatic volunteers. The authors found increased T2 values at the lateral zones of the acetabulum, with even further increases in the presence of an adjacent labral tear. Nishii *et al.* [85] investigated the change of cartilage T2 values with loading in patients with hip dysplasia. The decrease in cartilage T2 values was significantly greater in patients with DDH compared with asymptomatic volunteers.

MRI also allows assessment of the periarticular muscle mantle. It was previously shown that the iliocapsularis muscle, a small muscle overlying the anterior hip capsule, is hypertrophied in dysplastic hips. It was therefore suggested as an important dynamic stabilizer in the dysplastic hip [86]. Furthermore, an increased iliocapsularis-to-rectus-femoris ratio has been described as a secondary feature in DDH that can lead clinical decision making in hips with borderline hip dysplasia and a concomitant cam-type deformity to identify the predominant pathology [87]. It was shown that iliocapsularis-to-rectus-femoris ratio of 1:1 had a positive predictive value to distinguish dysplasia from protrusion of 89% for the diameter, 77% for the circumference, and 82% for the thickness of each muscle [87].

COMPUTER-ASSISTED PLANNING OF PAO

In the early years of PAO, conventional radiographs were based on analogue films. Radiographic parameters around the hip had to be obtained using rulers and markers. The introduction of digital radiography has simplified this evaluation. Furthermore, modern software applications were developed allowing to correct for pelvic tilt and rotation [52, 57, 88]. A validated computer analysis model (Hip^{2}Norm) exists that allows assessing acetabular parameters associated with DDH on AP pelvis radiographs [52, 57]. Selected landmarks on 2 D radiographic images such as the femoral head and acetabular centre, and the anterior and posterior wall contours are manually defined. The software reconstructs these landmarks in a 3 D coordinate system. Pelvic malorientation can be calibrated back to neutral. Pelvic tilt is adjusted by the pelvic inclination angle on a true lateral pelvic radiograph [89–91]. If no true lateral pelvic radiograph is available, the individual pelvic tilt can be estimated with the vertical distance between the sacrococcygeal joint and the upper border of the symphysis using standard values of this vertical distance from a normal population. This distance was shown to be 47 mm in females and 31.5 mm in males [56, 57].

Advances of multiplanar imaging modalities have opened a new field of 3D planning methods for PAO. As far back as 1988, Klaue *et al.* [46] introduced a computed

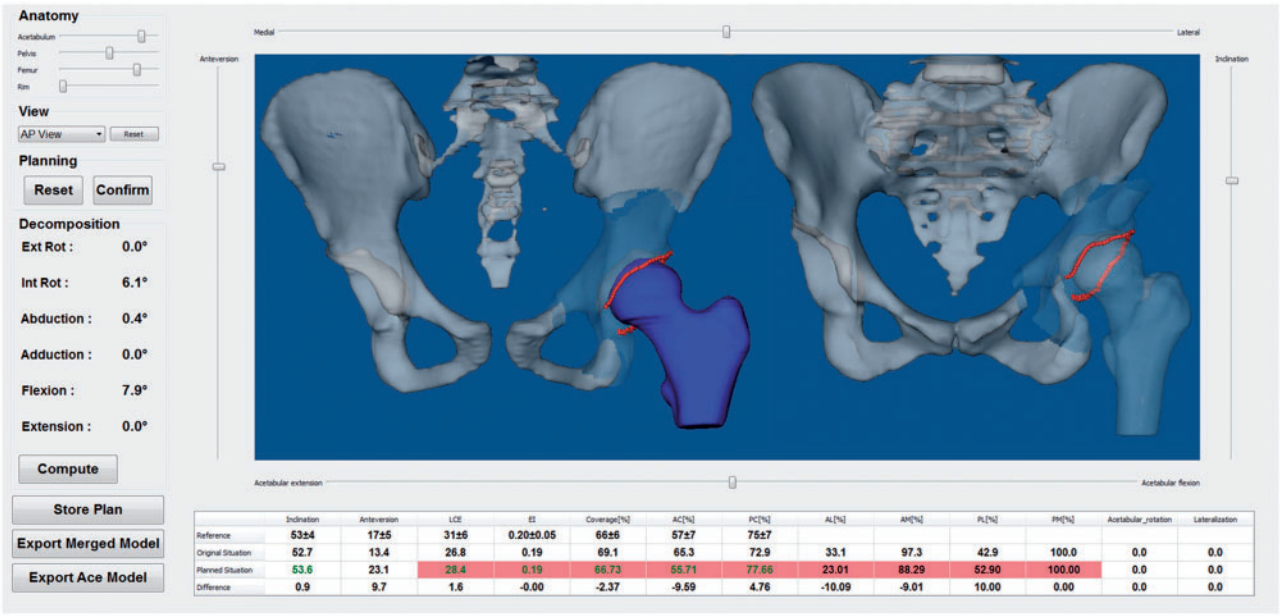

Fig. 6. Modern image segmentation applications based on CT-derived 3D models are available for preoperative planning of PAO. The application 'HipMotion' [88, 89] is based on a complex algorithm ultimately allowing for virtual 3D reorientation of the acetabulum in predefined increments. The software calculates conventional radiographic parameters in real time. After achieving desired degree of reorientation, virtual range of motion simulation allows to determine potential femoracetabular impingement conflicts after reorientation of the acetabulum.

tomography(CT)-based method for evaluating femoral coverage and joint congruency in hips undergoing PAO. This method was based on outlining the contours of the femoral head, the articulating surface area of the acetabulum and the acetabular cartilage on axial CT slices. The resulting lines at each assessed level were superimposed, creating a two dimensional topographical map defining the coverage of the femoral head. The authors also introduced rudimentary virtual reorientation manoeuvres to estimate the improvement of femoral head coverage after PAO [46]. Millis and Murphy reconstructed 3D CT scans and quantified femoral head containment by measuring classic geometric parameters in three dimensions [92]. Janzen *et al.* [93] measured centre edge angles on 3D CT reconstructed rotational sequences as reference values for preoperative planning for adult acetabular dysplasia. Dandachli *et al.* [94] introduced a CT based method to assess femoral head coverage, acetabular inclination and anteversion normalized to the anterior pelvic plane. With increasing technologic advances, an increasing number of modern image segmentation applications have become available for 3D preoperative planning. One of these applications utilizes 3 D models derived from CT data offering a diagnosis module for evaluating hip joint morphology including classic parameters (Table I), femoral head coverage and simulation of the reorientation [95–99]. The software algorithm is based on a feature for automated acetabular rim detection [96], definition of centre of rotation of the joint assuming equidistant cartilage thickness [98] and calculating the acetabular opening plane in relation to the anterior pelvic plane [99]. Virtual reorientation is achieved by excising a sphere over the acetabulum as a simplification of the actual osteotomies [100, 101]. The operator virtually performs stepwise increments of acetabular reorientation (flexion/extension, rotation and abduction/adduction; Fig. 6). The numeric change of the conventional radiographic parameters (Table I) and femoral head coverage is displayed in real time. After the desired degree of reorientation is achieved, range of motion analyses can be performed to recognize potential impingement conflicts [32, 64, 102, 103]. An alternative 3D planning tool not depending on proprietary third-party software is the Move Forward 3D Motion Simulation (Clinical Graphics; Zimmer Biomet) [104]. The software is based on CT or MR data and allows for 3D motion simulation and planning of the osteotomies. The software was initially developed for femoracetabular impingement motion analysis and collision detection of the osseous structures, however, a planning tool for PAO has recently been added as well. The segmentation process, editing of the 3D bone models, and motion analysis is exclusively executed by the company. An interactive PDF report is thereafter provided to the clinician [104].

Another approach to assess the effect of acetabular reorientation is based on methods assessing joint biomechanics. The commonality of these methods is that they rely on the estimation of peak contact pressures and contact areas. Different approaches are nowadays applied, such as discrete element analysis [105] or finite element analysis [106–109]. Potential benefits include the possibility of preoperative planning, visual feedback and intraoperative navigation [110]. One of the first studies was published by Hipp *et al.* [34] who reported a significant decrease of joint contact pressures after virtual reorientation of the acetabulum. Mechlenburg *et al.* [111] measured the area of load bearing before and after PAO based on a stereologic method. An improvement of the load bearing area was observed after PAO comparable to normal hips [111]. The research group around Armiger and Lepistö released a series of papers about a biomechanical guiding system (BGS) based on CT data for PAO [105, 112–115]. BGS combines preoperative planning with intraoperative fragment tracking, assessment of geometric parameters and real time biomechanics. In their most recent publication, the authors compared anatomic and biomechanical measurements obtained from BGS to manual, intraoperative measurements and measurements derived from postoperative CT in 12 PAO. BGS measurements of acetabular positioning were highly concordant with postoperative CT measurements while manual measurements during surgery revealed less accuracy [116].

SUMMARY AND CONCLUSION

Redirective, PAO render the potential for successful treatment of DDH in skeletally mature and immature patients. The common goal of these procedures is to relieve pain and to delay or prevent progression of OA to preserve the natural hip joint over time. Many factors associated with a good long-term result have been attributed to the accuracy of 3D re-orientation of the acetabulum [32]. As dysplastic acetabula exhibit an altered shape with a shallow socket and a decreased articular surface area, femoral coverage can only be restored to the best possible degree. Recognizing the patient-specific pathoanatomy requires thorough preoperative planning to achieve the best possible reorientation depending on the individual anatomic restraints. Next to clinical examination, routine preoperative planning consists of conventional radiography to identify specific acetabular and femoral radiographic parameters, MRI/MR-arthrogram to assess chondral and labral disease, and the status of the periarticular soft-tissues. CT may be performed to better assess the 3D osseous anatomy. Furthermore, modern computer-assisted methodologies allow for a dynamic assessment of the biomechanics and treatment simulation. However, implementation of these modern techniques in the daily routine requires further development prior to their widespread clinical application.

FUNDING

No funding was received for this article.

CONFLICT OF INTEREST STATEMENT

None declared.

REFERENCES

1. Murphy SB, Ganz R, Muller ME. The prognosis in untreated dysplasia of the hip. A study of radiographic factors that predict the outcome. *J Bone Joint Surg Am* 1995; **77**: 985–9.
2. Harris WH. Etiology of osteoarthritis of the hip. *Clin Orthop Relat Res* 1986; (**213**): 20–33.
3. Aronson J. Osteoarthritis of the young adult hip: etiology and treatment. *Instr Course Lect* 1986; **35**: 119–28.
4. Weinstein SL. Natural history of congenital hip dislocation (CDH) and hip dysplasia. *Clin Orthop Relat Res* 1987; (**225**): 62–76.
5. Migaud H, Spiers A, Gougeon F *et al.* Outcome of hip shelf arthroplasty in adults after a minimum of 15 years of follow-up. Long term results and analysis of failures of 56 dysplastic hips. *Rev Chir Orthop Reparatrice Appar Mot* 1995; **81**: 716–23.
6. Salter RB. Role of innominate osteotomy in the treatment of congenital dislocation and subluxation of the hip in the older child. *J Bone Joint Surg Am* 1966; **48**: 1413–39.
7. Chiari K. Pelvic osteotomy in hip arthroplasty. *Wien Med Wochenschr* 1953; **103**: 707–9.
8. Wagner H. Osteotomies for congenital hip dislocation. The hip. *Proceedings of the fourth open scientific meeting of the hip society*. St. Louis, CV Mosby, 1976; 45–66.
9. Ninomiya S, Tagawa H. Rotational acetabular osteotomy for the dysplastic hip. *J Bone Joint Surg Am* 1984; **66**: 430–6.
10. Tonnis D, Behrens K, Tscharani F. A modified technique of the triple pelvic osteotomy: early results. *J Pediatr Orthop* 1981; **1**: 241–9.
11. Carlioz H, Khouri N, Hulin P. Triple juxtacotyloid osteotomy. *Rev Chir Orthop Reparatrice Appar Mot* 1982; **68**: 497–501.
12. Ganz R, Klaue K, Vinh TS *et al.* A new periacetabular osteotomy for the treatment of hip dysplasias. Technique and preliminary results. *Clin Orthop Relat Res* 1988; **232**: 26–36.
13. Clohisy JC, Barrett SE, Gordon JE *et al.* Periacetabular osteotomy for the treatment of severe acetabular dysplasia. *J Bone Joint Surg Am* 2005; **87**: 254–9.
14. Clohisy JC, Barrett SE, Gordon JE *et al.* Periacetabular osteotomy in the treatment of severe acetabular dysplasia. *Surgical Technique. J Bone Joint Surg Am* 2006; **88**: 65–83.
15. Tannast M, Pfannebecker P, Schwab JM *et al.* Pelvic morphology differs in rotation and obliquity between developmental dysplasia of the hip and retroversion. *Clin Orthop Relat Res* 2012; **470**: 3297–305.

16. Ganz R, Horowitz K, Leunig M. Algorithm for femoral and periacetabular osteotomies in complex hip deformities. *Clin Orthop Relat Res* 2010; **468**: 3168–80.
17. Steppacher SD, Tannast M, Ganz R *et al*. Mean 20-year followup of Bernese periacetabular osteotomy. *Clin Orthop Relat Res* 2008; **466**: 1633–44.
18. Albers CE, Steppacher SD, Tannast M *et al*. Surgical Technique: Reverse Periacetabular Osteotomy. In: Nho SJ, Leunig M, Larson CM, Bedi A, Kelly BT (eds). *Hip Arthroscopy and Hip Joint Preservation Surgery*. New York, Springer, 2015; 638–51.
19. Tannast M, Hanke MS, Zheng G *et al*. What Are the Radiographic Reference Values for Acetabular Under- and Overcoverage? *Clin Orthop Relat Res* 2015; **473**: 1234–46.
20. Wiberg G. The anatomy and roentgenographic appearance of a normal hip joint. *Acta Chir Scand* 1939; **83**: 7–38.
21. Klaue K, Durnin CW, Ganz R. The acetabular rim syndrome. A clinical presentation of dysplasia of the hip. *J Bone Joint Surg Br* 1991; **73**: 423–9.
22. Brockwell J, O'Hara JN, Young DA. Acetabular Dysplasia: Aetiological Classification. In: McCarthy JC, Noble PC, Villar RN (eds). *Hip Joint Restoration*. New York, Springer, 2017; 631–42.
23. Pauwels F. *Biomechanics of the normal and diseased hip: theoretical foundation, technique and results of treatment*. Berlin, Heidelberg, New York, Springer, 1976.
24. Leunig M, Podeszwa D, Beck M *et al*. Magnetic resonance arthrography of labral disorders in hips with dysplasia and impingement. *Clin Orthop Relat Res* 2004; **418**: 74–80.
25. Cunningham T, Jessel R, Zurakowski D *et al*. Delayed gadolinium-enhanced magnetic resonance imaging of cartilage to predict early failure of Bernese periacetabular osteotomy for hip dysplasia. *J Bone Joint Surg Am* 2006; **88**: 1540–8.
26. Hingsammer AM, Kalish LA, Stelzeneder D *et al*. Does periacetabular osteotomy for hip dysplasia modulate cartilage biochemistry? *J Bone Joint Surg Am* 2015; **97**: 544–50.
27. Kim SD, Jessel R, Zurakowski D *et al*. Anterior delayed gadolinium-enhanced MRI of cartilage values predict joint failure after periacetabular osteotomy. *Clin Orthop Relat Res* 2012; **470**: 3332–41.
28. Ganz R, Parvizi J, Beck M *et al*. Femoroacetabular impingement: a cause for osteoarthritis of the hip. *Clin Orthop Relat Res* 2003; **417**: 112–20.
29. Fujii M, Nakashima Y, Yamamoto T *et al*. Acetabular retroversion in developmental dysplasia of the hip. *J Bone Joint Surg Am* 2010; **92**: 895–903.
30. Li PL, Ganz R. Morphologic features of congenital acetabular dysplasia: one. *In Six Is Retroverted. Clin Orthop Relat Res* 2003; **416**: 245–53.
31. Reynolds D, Lucas J, Klaue K. Retroversion of the acetabulum. A cause of hip pain. *J Bone Joint Surg Br* 1999; **81**: 281–8.
32. Albers CE, Steppacher SD, Ganz R *et al*. Impingement adversely affects 10-year survivorship after periacetabular osteotomy for DDH. *Clin Orthop Relat Res* 2013; **471**: 1602–14.
33. Hartig-Andreasen C, Troelsen A, Thillemann TM *et al*. Risk factors for the need of hip arthroscopy following periacetabular osteotomy. *J Hip Preserv Surg* 2015; **2**: 374–84.
34. Hipp JA, Sugano N, Millis MB *et al*. Planning acetabular redirection osteotomies based on joint contact pressures. *Clin Orthop Relat Res* 1999; **364**: 134–43.
35. Steppacher SD, Lerch TD, Gharanizadeh K *et al*. Size and shape of the lunate surface in different types of pincer impingement: theoretical implications for surgical therapy. *Osteoarthritis Cartilage* 2014; **22**: 951–8.
36. Lerch TD, Steppacher SD, Liechti EF *et al*. One-third of hips after periacetabular osteotomy survive 30 years with good clinical results, no progression of arthritis, or conversion to THA. *Clin Orthop Relat Res* 2017; **475**: 1154–68.
37. Yasunaga Y, Takahashi K, Ochi M *et al*. Rotational acetabular osteotomy in patients forty-six years of age or older: comparison with younger patients. *J Bone Joint Surg Am* 2003; **85-A**: 266–72.
38. Teratani T, Naito M, Kiyama T *et al*. Periacetabular osteotomy in patients fifty years of age or older. *J Bone Joint Surg Am* 2010; **92**: 31–41.
39. Okano K, Enomoto H, Osaki M *et al*. Rotational acetabular osteotomy for advanced osteoarthritis secondary to developmental dysplasia of the hip. *J Bone Joint Surg Br* 2008; **90**: 23–6.
40. Tannast M, Siebenrock KA, Anderson SE. Femoroacetabular impingement: radiographic diagnosis-what the radiologist should know. *AJR Am J Roentgenol* 2007; **188**: 1540–52.
41. Clohisy JC, Carlisle JC, Beaule PE *et al*. A systematic approach to the plain radiographic evaluation of the young adult hip. *J Bone Joint Surg Am* 2008; **90**(Suppl 4): 47–66.
42. Lauenstein C. Nachweis der 'Kocherschen Verbiegung' des Schenkelhalses bei der Coxa vara durch Röntgenstrahlen. *Fortschr Röntgenstr* 1901; **4**: 61–4.
43. Dunn DM. Anteversion of the neck of the femur; a method of measurement. *J Bone Joint Surg Br* 1952; **34-B**: 181–6.
44. Rippstein J. Determination of the antetorsion of the femur neck by means of two x-ray pictures. *Z Orthop Ihre Grenzgeb* 1955; **86**: 345–60.
45. Lequesne M, de S. False profile of the pelvis. A new radiographic incidence for the study of the hip. Its use in dysplasias and different coxopathies. *Rev Rhum Mal Osteoartic* 1961; **28**: 643–52.
46. Klaue K, Wallin A, Ganz R. CT evaluation of coverage and congruency of the hip prior to osteotomy. *Clin Orthop Relat Res* 1988; **232**: 15–25.
47. Tönnis D, Heinecke A. Acetabular and femoral anteversion: relationship with osteoarthritis of the hip. *J Bone Joint Surg Am* 1999; **81**: 1747–70.
48. Siebenrock KA, Kistler L, Schwab JM *et al*. The acetabular wall index for assessing anteroposterior femoral head coverage in symptomatic patients. *Clin Orthop Relat Res* 2012; **470**: 3355–60.
49. Kalberer F, Sierra RJ, Madan SS *et al*. Ischial spine projection into the pelvis: a new sign for acetabular retroversion. *Clin Orthop Relat Res* 2008; **466**: 677–83.
50. Burckhardt K. Theoretical Study to the Sub-project 'Interactive Software for 2D and 3D Standardization of Pelvic Radiographs and CT-Scans for Accurate Evaluation of Hip Joint Morphology' under CO-ME Project 4. Swiss Federal Institute of Technology. 2003; 267.

51. Tannast M, Fritsch S, Zheng G *et al*. Which radiographic hip parameters do not have to be corrected for pelvic rotation and tilt? *Clin Orthop Relat Res* 2015; **473**: 1255–66.
52. Tannast M, Mistry S, Steppacher SD *et al*. Radiographic analysis of femoroacetabular impingement with Hip2Norm-reliable and validated. *J Orthop Res* 2008; **26**: 1199–205.
53. Tannast M, Zheng G, Anderegg C *et al*. Tilt and rotation correction of acetabular version on pelvic radiographs. *Clin Orthop Relat Res* 2005; **438**: 182–90.
54. Steppacher SD, Albers CE, Tannast M *et al*. Plain radiographic evaluation of the hip. In: Nho SH, Leunig M, Larson CM, Bedi A, Kelly BT (eds). *Hip Arthroscopy and Hip Joint Preservation Surgery*. New York, Heidelberg, Dordrecht, London, Springer, 2015; 33–51.
55. Tannast M, Siebenrock KA. Imaging: Plain Radiographs. In: Sekiya JK, Safran MR, Ranawat AS, Leunig M, (eds). *Techniques in Hip Arthroscopy and Joint Preservation*. Philadelphia: Elsevier Saunders, 2011; 23-4.
56. Siebenrock KA, Kalbermatten DF, Ganz R. Effect of pelvic tilt on acetabular retroversion: a study of pelves from cadavers. *Clin Orthop Relat Res* 2003; **407**: 241–8.
57. Zheng G, Tannast M, Anderegg C *et al*. Hip2Norm: an object-oriented cross-platform program for 3D analysis of hip joint morphology using 2D pelvic radiographs. *Comput Methods Programs Biomed* 2007; **87**: 36–45.
58. Tönnis D. Gerneral radiography of the hip joint. In: Tönnis D (ed). *Congenital Dysplasia, Dislocation of the Hip*. New York, NY, Springer, 1987, 100–42.
59. Idelberger K, Frank A. A new method for determination of the angle of the pevic acetabulum in child and in adult. *Z Orthop Ihre Grenzgeb* 1952; **82**: 571–7.
60. Jackson TJ, Estess AA, Adamson GJ. Supine and standing AP pelvis radiographs in the evaluation of pincer femoroacetabular impingement. *Clin Orthop Relat Res* 2016; **474**: 1692–6.
61. Novais EN, Duncan S, Nepple J *et al*. Do radiographic parameters of dysplasia improve to normal ranges after bernese periacetabular osteotomy? *Clin Orthop Relat Res* 2017; **475**: 1120–7.
62. Matta JM, Stover MD, Siebenrock K. Periacetabular osteotomy through the Smith-Petersen approach. *Clin Orthop Relat Res* 1999; **363**: 21–32.
63. Mast JW, Brunner RL, Zebrack J. Recognizing acetabular version in the radiographic presentation of hip dysplasia. *Clin Orthop Relat Res* 2004; **418**: 48–53.
64. Steppacher SD, Tannast M, Werlen S *et al*. Femoral morphology differs between deficient and excessive acetabular coverage. *Clin Orthop Relat Res* 2008; **466**: 782–90.
65. Ziebarth K, Balakumar J, Domayer S *et al*. Bernese periacetabular osteotomy in males: is there an increased risk of femoroacetabular impingement (FAI) after Bernese periacetabular osteotomy? *Clin Orthop Relat Res* 2011; **469**: 447–53.
66. Notzli HP, Wyss TF, Stoecklin CH *et al*. The contour of the femoral head-neck junction as a predictor for the rick of anterior impingement. *J Bone Joint Surg Br* 2002; **84**: 556–60.
67. Ito K, Minka MA, 2nd, Leunig M *et al*. Femoroacetabular impingement and the cam-effect. A MRI-based quantitative anatomical study of the femoral head-neck offset. *J Bone Joint Surg Br* 2001; **83**: 171–6.
68. Stulberg SD, Cordell LD, Harris WH *et al*. Unrecognized childhood hip disease: a major cause of idiopathic osteoarthritis of the hip. In: *The Hip. Proceedings of the 3rd Meeting of the Hip Society*. St Louis, CV Mosby Co, 1975; 121–8.
69. Murphy SB, Simon SR, Kijewski PK *et al*. Femoral anteversion. *J Bone Joint Surg Am* 1987; **69**: 1169–76.
70. Hersche O, Casillas M, Ganz R. Indications for intertrochanteric osteotomy after periacetabular osteotomy for adult hip dysplasia. *Clin Orthop Relat Res* 1998; **347**: 19-26.
71. Saupe N, Zanetti M, Pfirrmann CW *et al*. Pain and other side effects after MR arthrography: prospective evaluation in 1085 patients. *Radiology* 2009; **250**: 830–8.
72. Sutter R, Zubler V, Hoffmann A *et al*. Hip MRI: how useful is intraarticular contrast material for evaluating surgically proven lesions of the labrum and articular cartilage? AJR. *Am J Roentgenol* 2014; **202**: 160–9.
73. Magee T. Comparison of 3.0-T MR vs 3.0-T MR arthrography of the hip for detection of acetabular labral tears and chondral defects in the same patient population. *Br J Radiol* 2015; **88**: 20140817.
74. Sankar WN, Beaule PE, Clohisy JC *et al*. Labral morphologic characteristics in patients with symptomatic acetabular dysplasia. *Am J Sports Med* 2015; **43**: 2152–6.
75. Beck M, Kalhor M, Leunig M *et al*. Hip morphology influences the pattern of damage to the acetabular cartilage: femoroacetabular impingement as a cause of early osteoarthritis of the hip. *J Bone Joint Surg Br* 2005; **87**: 1012–8.
76. Garabekyan T, Ashwell Z, Chadayammuri V *et al*. Lateral acetabular coverage predicts the size of the hip labrum. *Am J Sports Med* 2016; **44**: 1582–9.
77. Wells J, Millis M, Kim YJ *et al*. Survivorship of the Bernese periacetabular osteotomy: what factors are associated with long-term failure? *Clin Orthop Relat Res* 2017; **475**: 396–405.
78. Potter HG, Schachar J. High resolution noncontrast MRI of the hip. *J Magn Reson Imaging* 2010; **31**: 268–78.
79. Gold SL, Burge AJ, Potter HG. MRI of hip cartilage: joint morphology, structure, and composition. *Clin Orthop Relat Res* 2012; **470**: 3321–31.
80. Bittersohl B, Hosalkar HS, Hesper T *et al*. Advanced imaging in femoroacetabular impingement: current state and future prospects. *Front Surg* 2015; **2**: 34.
81. Hingsammer A, Chan J, Kalish LA *et al*. Is the damage of cartilage a global or localized phenomenon in hip dysplasia, measured by dGEMRIC? *Clin Orthop Relat Res* 2013; **471**: 301–7.
82. Nieminen MT, Rieppo J, Toyras J *et al*. T2 relaxation reveals spatial collagen architecture in articular cartilage: a comparative quantitative MRI and polarized light microscopic study. *Magn Reson Med* 2001; **46**: 487–93.
83. Liess C, Lusse S, Karger N *et al*. Detection of changes in cartilage water content using MRI T2-mapping in vivo. *Osteoarthritis Cartilage* 2002; **10**: 907–13.
84. Hamada H, Nishii T, Tamura S *et al*. Three dimensional distribution of hip cartilage t2 mapping assessed by radial mr imaging: comparison between healthy volunteers and patients with hip dysplasia. *Osteoarthritis Cartilage* 2014; **22**: 353–4.

85. Nishii T, Shiomi T, Tanaka H *et al*. Loaded cartilage T2 mapping in patients with hip dysplasia. *Radiology* 2010; **256**: 955–65.
86. Babst D, Steppacher SD, Ganz R *et al*. The iliocapsularis muscle: an important stabilizer in the dysplastic hip. *Clin Orthop Relat Res* 2011; **469**: 1728–34.
87. Haefeli PC, Steppacher SD, Babst D *et al*. An increased iliocapsularis-to-rectus-femoris ratio is suggestive for instability in borderline hips. *Clin Orthop Relat Res* 2015; **473**: 3725–34.
88. Dutoit M, Zambelli PY. Simplified 3D-evaluation of periacetabular osteotomy. *Acta Orthop Belg* 1999; **65**: 288–94.
89. Drenckhahn D, Eckstein F. Untere extremität. In: Drenckhahn D (ed.). *Benninghoff Anatomie.* München, Urban & Fischer, 2003.
90. Lierse W. *Praktische Anatomie*. Lantz T, Wachsmuth W, (eds.). Berlin, Springer, 1988.
91. Williams PL. The skeleton of the lower limb. In: Williams PL, Warkick R, Dyson M, Bannister LH, (eds.). *Gray's Anatomy*. Edinburgh, UK, Churchill Livingstone, 1989.
92. Millis MB, Murphy SB. Use of computed tomographic reconstruction in planning osteotomies of the hip. *Clin Orthop Relat Res* 1992; **274**: 154–9.
93. Janzen DL, Aippersbach SE, Munk PL *et al*. Three-dimensional CT measurement of adult acetabular dysplasia: technique, preliminary results in normal subjects, and potential applications. *Skeletal Radiol* 1998; **27**: 352–8.
94. Dandachli W, Kannan V, Richards R *et al*. Analysis of cover of the femoral head in normal and dysplastic hips: new CT-based technique. *J Bone Joint Surg Br* 2008; **90**: 1428–34.
95. Ecker TM, Puls M, Steppacher SD *et al*. Computer-assisted femoral head-neck osteochondroplasty using a surgical milling device an in vitro accuracy study. *J Arthroplasty* 2012; **27**: 310–6.
96. Puls M, Ecker TM, Steppacher SD *et al*. Automated detection of the osseous acetabular rim using three-dimensional models of the pelvis. *Comput Biol Med* 2011; **41**: 285–91.
97. Rudolph T, Puls M, Anderegg C *et al*. MARVIN: a medical research application framework based on open source software. *Comput Methods Programs Biomed* 2008; **91**: 165–74.
98. Puls M, Ecker TM, Tannast M *et al*. The Equidistant method - a novel hip joint simulation algorithm for detection of femoroacetabular impingement. *Comput Aided Surg* 2010; **15**: 75–82.
99. Tannast M, Kubiak-Langer M, Langlotz F *et al*. Noninvasive three-dimensional assessment of femoroacetabular impingement. *J Orthop Res* 2007; **25**: 122–31.
100. Liu L, Ecker TM, Schumann S *et al*. Computer assisted planning and navigation of periacetabular osteotomy with range of motion optimization. In: Zheng G, Liao H, Jannin P, Cattin P, Lee S-L, (eds). *Medical Imaging and Augmented Reality*. Switzerland, Springer International Publishing, 2016; 15–26.
101. Liu L, Zheng G, Bastian JD *et al*. Periacetabular osteotomy through the pararectus approach: technical feasibility and control of fragment mobility by a validated surgical navigation system in a cadaver experiment. *Int Orthop* 2015; **40**: 1389–96.
102. Steppacher SD, Zurmuhle CA, Puls M *et al*. Periacetabular osteotomy restores the typically excessive range of motion in dysplastic hips with a spherical head. *Clin Orthop Relat Res* 2015; **473**: 1404–16.
103. Kubiak-Langer M, Tannast M, Murphy SB *et al*. Range of motion in anterior femoroacetabular impingement. *Clin Orthop Relat Res* 2007; **458**: 117–24.
104. ClinicalGraphics. *Viewing guide for Move Forward™ Hip Dysplasia (PAO) Reports*. Delft, Netherlands, Zimmer Biomet.
105. Armand M, Lepisto J, Tallroth K *et al*. Outcome of periacetabular osteotomy: joint contact pressure calculation using standing AP radiographs, 12 patients followed for average 2 years. *Acta Orthop* 2005; **76**: 303–13.
106. Zhao X, Chosa E, Totoribe K *et al*. Effect of periacetabular osteotomy for acetabular dysplasia clarified by three-dimensional finite element analysis. *J Orthop Sci* 2010; **15**: 632–40.
107. Zou Z, Chavez-Arreola A, Mandal P *et al*. Optimization of the position of the acetabulum in a ganz periacetabular osteotomy by finite element analysis. *J Orthop Res* 2013; **31**: 472–9.
108. Harris MD, Anderson AE, Henak CR *et al*. Finite element prediction of cartilage contact stresses in normal human hips. *J Orthop Res* 2012; **30**: 1133–9.
109. Liu L, Ecker TM, Schumann S *et al*. Evaluation of constant thickness cartilage models vs. patient specific cartilage models for an optimized computer-assisted planning of periacetabular osteotomy. *PLoS One* 2016; **11**: e0146452.
110. Pflugi S, Liu L, Ecker TM *et al*. A cost-effective surgical navigation solution for periacetabular osteotomy (PAO) surgery. *Int J Comput Assist Radiol Surg* 2016; **11**: 271–80.
111. Mechlenburg I, Nyengaard JR, Romer L *et al*. Changes in load-bearing area after Ganz periacetabular osteotomy evaluated by multislice CT scanning and stereology. *Acta Orthop Scand* 2004; **75**: 147–53.
112. Armiger RS, Armand M, Lepisto J *et al*. Evaluation of a computerized measurement technique for joint alignment before and during periacetabular osteotomy. *Comput Aided Surg* 2007; **12**: 215–24.
113. Armiger RS, Armand M, Tallroth K *et al*. Three-dimensional mechanical evaluation of joint contact pressure in 12 periacetabular osteotomy patients with 10-year follow-up. *Acta Orthop* 2009; **80**: 155–61.
114. Lepisto J, Armand M, Armiger RS. Periacetabular osteotomy in adult hip dysplasia - developing a computer aided real-time biomechanical guiding system (BGS). *Suom Ortoped Traumatol* 2008; **31**: 186–90.
115. Murphy RJ, Armiger RS, Lepisto J *et al*. Development of a biomechanical guidance system for periacetabular osteotomy. *Int J Comput Assist Radiol Surg* 2015; **10**: 497–508.
116. Murphy RJ, Armiger RS, Lepisto J *et al*. Clinical evaluation of a biomechanical guidance system for periacetabular osteotomy. *J Orthop Surg Res* 2016; **11**: 36.
117. Sharp IK. Acetabular dysplasia: the acetabular angle. *J Bone Joint Surg Br* 1961; **43**: 268–7.
118. Siebenrock KA, Steppacher SD, Albers CE *et al*. Diagnosis and management of developmental dysplasia of the hip from triradiate closure through young adulthood. *Instr Course Lect* 2014; **63**: 325–34.